Journal of Ceramic Processing Research. Vol. 5, No. 3, pp. 214~222 (2004)

J O U R N A L O F
Ceramic Processing Research

Responses of an atmospheric plasma sprayed (APS) alumina-titania coating to scratch wear

Hanshin Choi[a],* and Changhee Lee[b]
[a]*Nono Materials Team, Korea Institute of Industrial Technology, Incheon 404-254, Korea*
[b]*Neomaterials and Hybrid Process Lab., Hanyang University, Seoul 133-791, Korea*

An alumina-titania composite coating was produced using a thermal plasma spraying coating process. As-sprayed coating microstructures were observed using scanning electron microscopy and energy dispersive spectroscopy. A scratch test was conducted on the finely-polished coating under conditions of constant loading speed and moving rate. Acoustic emissions as well as scratching coefficient were measured during scratching. During the cyclic scratching, the APS coating showed fatigue. The transition from plastic deformation to fracture was time-dependent and it was also accelerated with an increase of the applied normal load. During plastic deformation, fine wear debris resulted from grain crushing while the flake-like large debris was formed due to the initiation and propagation of microcracks during fracturing. The major defects in the microstructures gave different wear debris. Fine particle formation was promoted by discontinuities whereas flake debris was mainly due to the intersplat pores between splats and vertical cracks in the splat.

Key words: Alumina-titania, Atmospheric plasma spraying, Scratch test, Defective microstructure, Wear.

Introduction

The atmospheric plasma spraying (APS) process is one of the most versatile coating processes for industrial applications [1]. Due to the unique properties of the thermal plasma [2], engineering ceramic materials as well as refractory materials can be sprayed. Like other thermal spraying processes, the powder feedstock materials are injected into the thermal plasma jet downstream, and they are accelerated and heated to reach a certain molten state during flight [3]. The APS coating is composed of the build-up of individual splats that are the flattened and solidified impacting particles [4]. Intrinsically defective microstructures, containing defects such as pores and cracks are formed during processing. Futhermore, the coating properties are largely dependent on the coating microstructures including these defects [5-7].

Alumina is a well-developed engineering ceramic material for resisting wear which is used within various industrial fields. However, its lower fracture toughness due to a higher sensitivity to cracking has been a major drawback. In order to improve the fracture toughness of alumina, titania is introduced to form a composite material. As the titania content is increased, the fracture toughness is increased while the microhardness is decreased [8]. Aside from the chemistry, the mechanical properties of alumina-titania composite also depend on the process parameters [9], powder manufacturing method [10], and particle size [8]. In our previous work, the pin-on-plate wear behaviors of alumina-titania APS coatings were evaluated and the time-dependent transition of the weight loss was observed to depend strongly on the coating microstructure. In order to study this transition behavior in more detail, a scratch wear test [11-13] was introduced in this study. During the cyclic scratching, physical and ceramographical changes were observed.

*Corresponding author:
Tel : +82-2-2290-0388
Fax: +82-2-2290-0389
E-mail: chlee@hanyang.ac.kr

Experimental procedure

Commercial grade clad feedstock was deposited onto AISI 304 stainless steel using an atmospheric thermal plasma spraying process. The characteristics of the powder feedstock were observed using scanning electron microscopy and x-ray diffraction. An argon and hydrogen gas mixture [100SCFH Ar at 690 kPa-20SCFH H_2] was used for the plasma gas. The spraying distance from the nozzle exit to the substrate was 100 mm. The arc current was kept at 500A during processing. Before charging the feedstock material, the substrate was preheated using the plasma plume. Vickers microhardness was measured on the surface under a 300 gf load for 15 s. The Vickers microhardness of the as-sprayed coating was Hv 1064 [SD = 124]. A scratch test was conducted on the fine-polished to a 0.3 μm-diamond suspension coatings using Swiss Center for Electronics and Microtechnology (CSEM). The loading condition was such that the normal load was progressively

Table 1. Characteristics of the alumina-titania powder feedstock

Nominal chemistry	Phase Composition	Shape	Powder size	Manufacturing method
Al_2O_3-13 wt.%TiO_2	α-Al_2O_3 anatase-TiO_2	Angular & blocky	-30+5 μm	Clad

increased at a rate of 30 Nm^{-1} and the specimen travel rate was 20 mm m^{-1}. Cyclic scratching was applied in the identical direction and path to 20 repeated scratchings. After scratching, the morphology of the scratch was examined using scanning electron microscopy and energy dispersive spectroscopy. In order to examine the morphological changes due to the accumulation of the scratching cycles, a cross section was prepared using a tripod polishing kit.

Results

Characteristics of the feedstock materials are summarized in the Table 1. The clad powder showed non-uniformity in elemental distribution.

Typical microstructures of as-sprayed coatings can be seen in Fig. 1. An APS coating is produced by the successive build-ups of a great number of splats. During the deposition of a molten particle, the energy conversion processes accompany the particle flattening with viscous energy dissipation and solidification, and cooling with the release of thermal energy. Therefore, the splat morphology is largely dependent on these phenomena; well-defined disc-like splats through to highly splashed splats can be formed according to the energy state of the impacting particle and substrate temperature as can be seen in (a). An alternate lamellar structure can be noted in the back-scattered cross section image (b). Through energy dispersive spectroscopy, it could be observed that the bright region was rich in Ti whereas the dark region was rich in Al. The coating properties are largely dependent upon the coating microstructures. In particular, the defects in the microstructures in the thermally sprayed coatings have detrimental effects on the mechanical properties. Typical defects were pores and cracks. A large number of pores can be seen in the as-sprayed coatings such as intersplat pores and intrasplat pores. While the intersplat pores generally result from the poor contact between splats and/or the insufficient filling of the pre-existing interstices by a subsequently deposited molten particle, the intrasplat pore is due to entrapped gas. On the other hand, the macro/micro-cracks result from thermal stresses such as quench stresses and thermal expansion mismatch-induced stresses. Macro-cracking was hardly observed in the coatings. However, a quenched tensile stress resulted in a vertical crack within the splat as shown in (d). In some cases, spontaneous spallation was found within the splat due to the inter-linkage of the vertical cracks. Also, unmelted particles were present

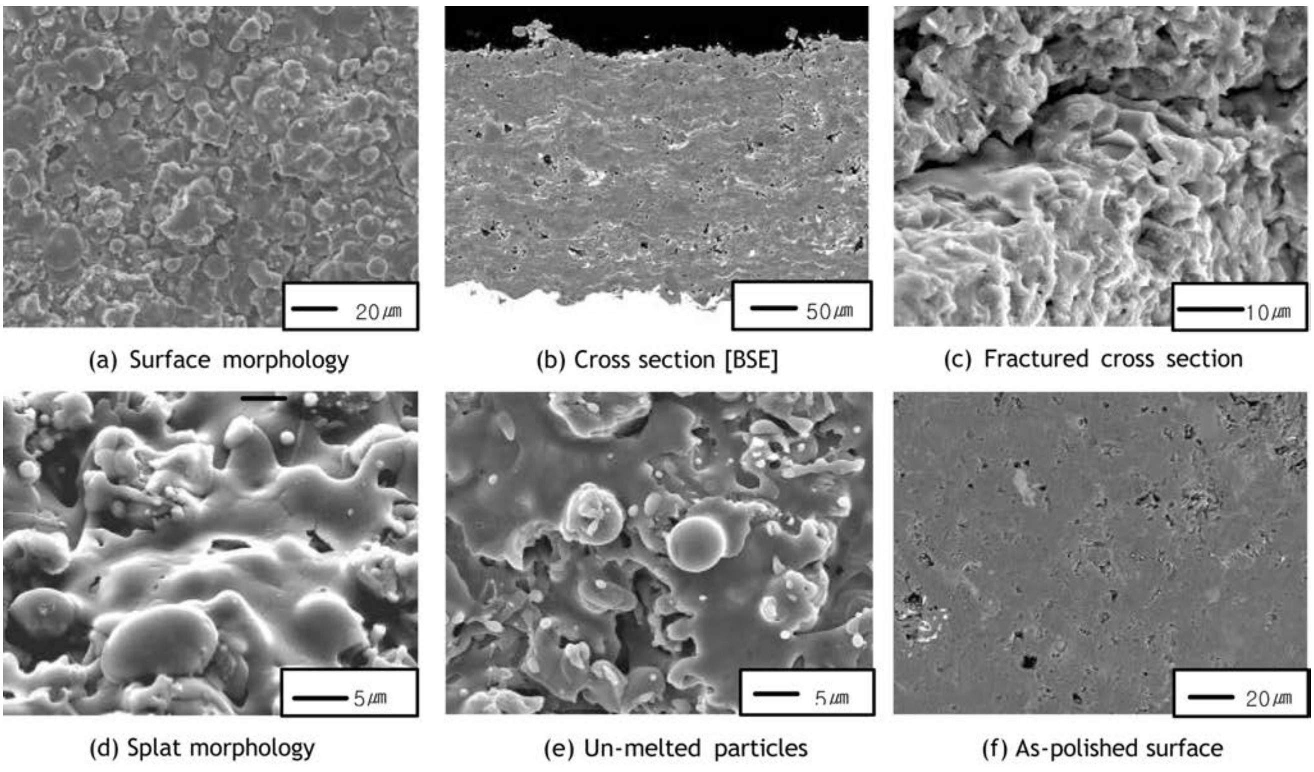

Fig. 1. Coating microstructure of the as-sprayed alumina-titania coating.

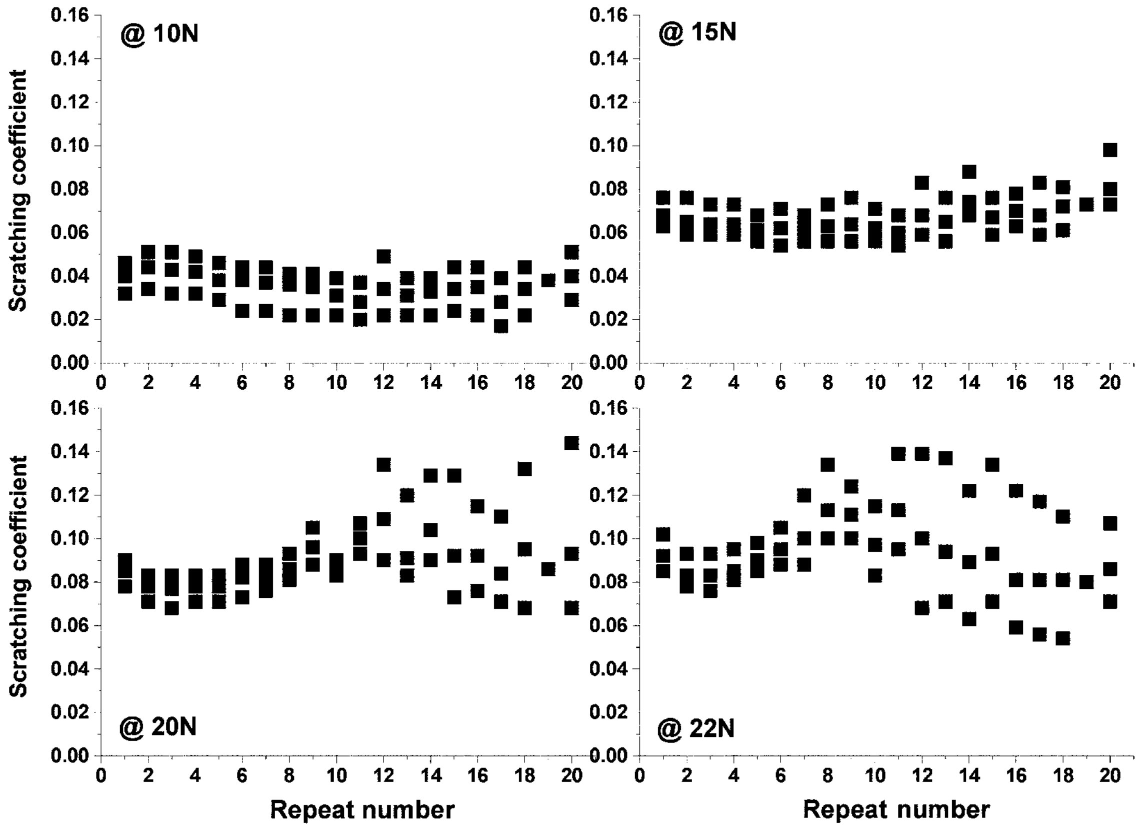

Fig. 2. Scratching coefficient variations during the cyclic scratching.

in the coating due to insufficient melting at the moment of impact as shown in (e). Unmelted particles in the sprayed coating are known to play a shadow effect against the particle streamline. Futher, fine particles are observed around splats. These fine particles resulted from the splashing of the flattening liquid droplet. Image (f) shows the surface morphology of an as-polished coating. The number density of pores is relatively high in some local regions the as same as for the improperly flattened zone in our previous work [14]. Rapid solidification processes could be deduced from the extinction of the titania peak and the high volume fraction of the γ-alumina phase in the coating as determined by the X-ray diffraction.

Evolution of the scratching coefficient with cycle accumulation is shown in Fig. 2. Three data points shown at each repeat number are the maximum value, the mean value, and the minimum value, respectively. As the applied normal load was increased, the mean scratching coefficient increased. The initial decrease of the scratching coefficient was followed by an increase with a further increase of the repeat scratch number. This trend seemed to be accelerated with size of the normal load. At higher normal loads, the data scatter was enhanced and the threshold repeat number showings a large scatter was shortened with the applied load. This scattering in the scratching coefficient implies that there was a significant change in the response of the coating material to the moving indenter.

The effect of the normal load on the scratch morphology during cyclic scratching can be seen in Fig. 3. When the normal load was increased, the scratch width increased. Also some morphological transitions can be observed above a normal load of 20N after a 10-repeated cycle. At the normal loads of 10N and 18N, the fragmented fine wear debris was examined along the indenter travel path and at the edge of the scratch. The severe plastic deformation due to the inelastic mass flow results in a decrease of the defect densities. However, a microcrack vertical to the indent moving direction can be observed in (c) and (d). Moreover, spalled flake-like debris can be found at a normal load of 22N.

Meanwhile, the number of scratch repeats also had an influence on the scratch morphology as shown in Fig. 4 and Fig. 5. In Fig. 4, there is no big change observed except that the scratch width is enlarged and the fine particle population has increased with the number of repeats. However, severe deformation was attained within a short period of repeated scratching. Cracking and spalling were also present in the scratch after 10 passes. As the pass number was further increased, overall spalling of the scratch path was observed as can be seen in Fig. 5(d).

Figure 6 shows the correlation between the acoustic emission signal and the variation of the scratching

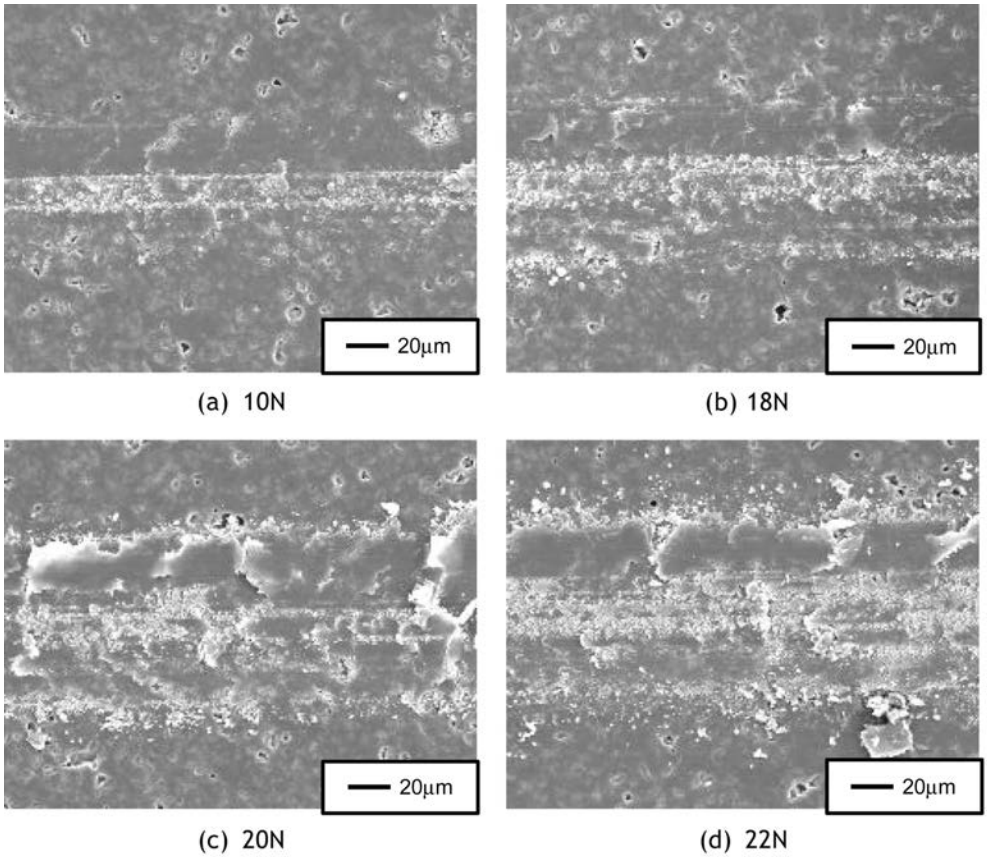

Fig. 3. Surface morphology of the as-scratched coating for 10 scratch passes.

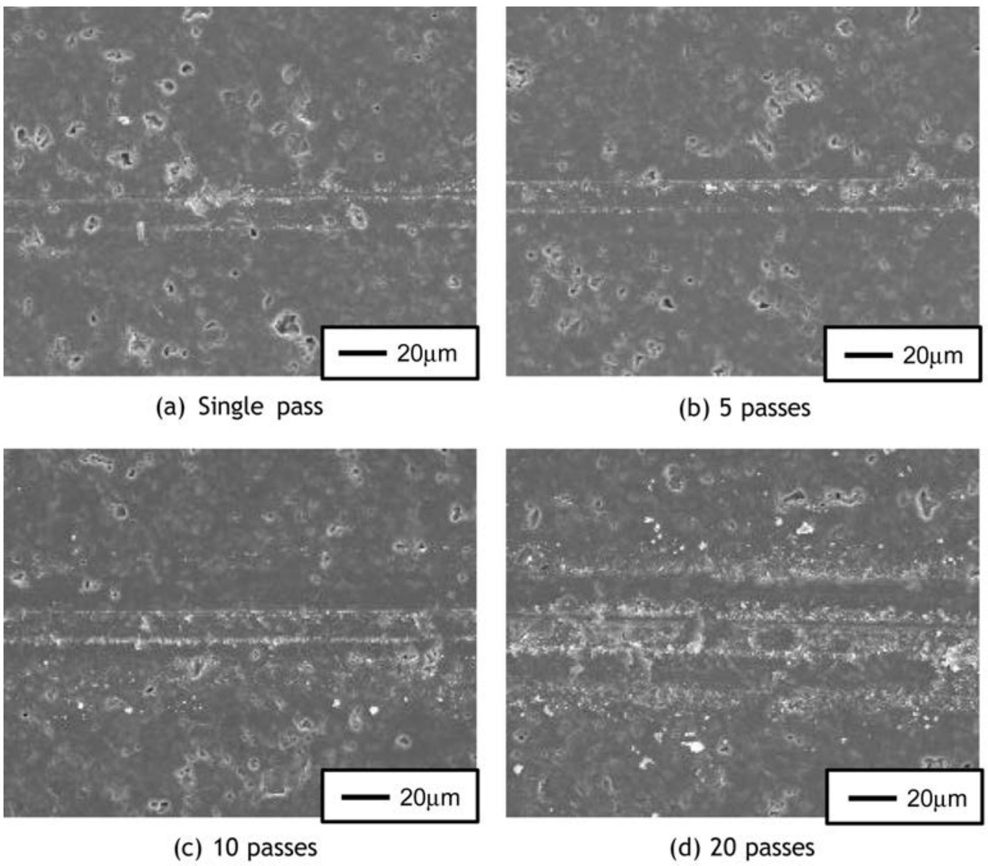

Fig. 4. Surface morphology of the as-scratched coating at a normal load of 10 N.

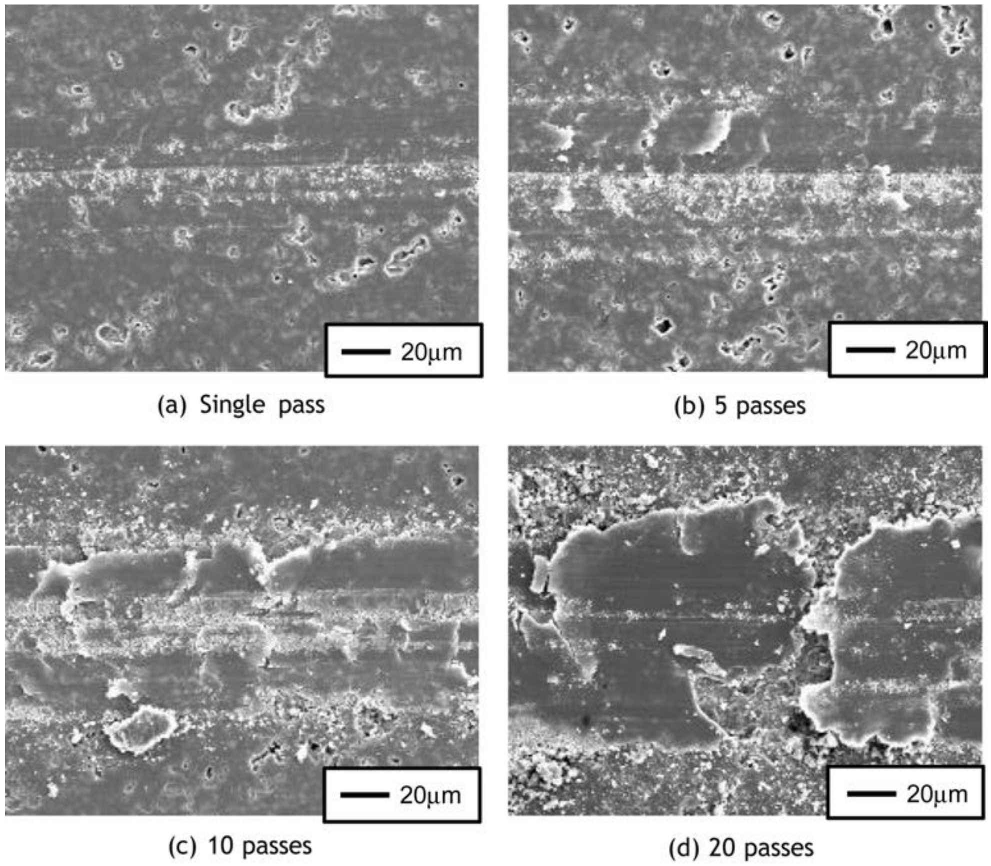

Fig. 5. Surface morphology of the as-scratched coating at a normal load of 22 N.

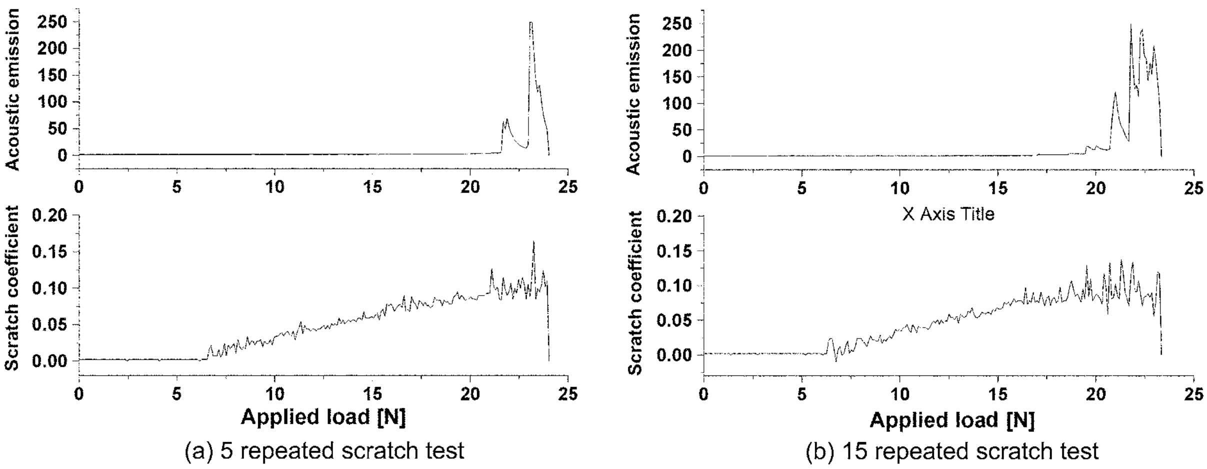

Fig. 6. Acoustic emission and scratch coefficient according to the number of passes.

coefficient. Sharp peaks were observed coincident with an increase in the fluctuation of the scratching coefficient. In addition to the change in the microstructural morphology, this result confirmed that the change in the response of the coating to the scratching indenter was mainly due to microcracking and fractures on the scratching path.

In summary, the morphological change of the scratch was largely dependent on the number of scratch passes and the normal load. As the number of scratch passes increased, the transition from plastic deformation to fracture occurred due to microcracking along the inter-splat boundaries. This transition time could be shortened with an increase of the normal load.

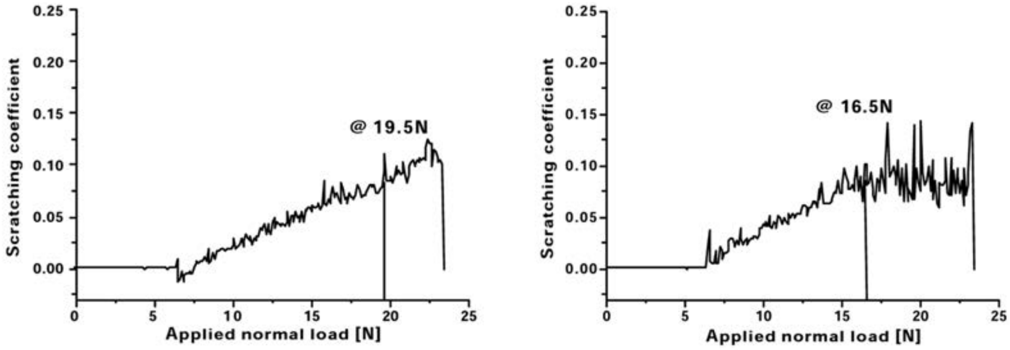

(a) Scratch coefficient at 10th scratch pass (b) Scratch coefficient at 20th scratch pass

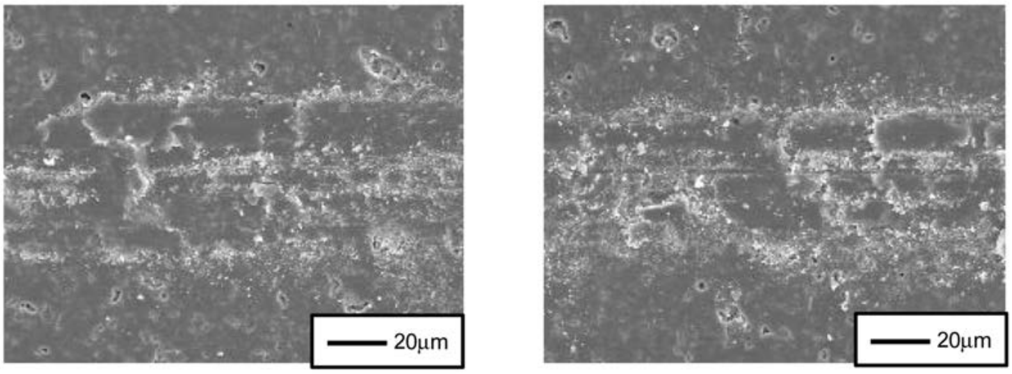

(c) Surface morphology at 19.5N of (a) (d) Surface morphology at 16.5N of (b)

Fig. 7. Correlation of acoustic emission behavior with scratch morphology.

Discussion

A morphological transition in the scratch was correlated with a change in the scratching coefficient. The transition from severe plastic deformation to fracture in the scratch can be detected with an increase in the fluctuation of the scratching coefficient as shown in Fig. 7. Thus, the enhanced stick-slip like fluctuation in the scratching coefficient is considered to relate to microcracking in the scratching path.

Fine wear debris observed along the centerline and edge of the scratch seemed to be due to grain crushing after severe plastic deformation. The improperly flattened zone, characterized by the high local pore density, in the coating might promote grain crushing as shown in Fig. 8. In the case of region A where the improperly flattened zone has been located on the centerline of the cyclic scratch, the number density of the fine wear debris is higher around it without sufficient closure of the pore. Similar to region A, the improperly flattened zone along the scratch edge plays a nucleations role in the fine wear debris. In fact, all the discontinuities such as isolated pores and improperly flattened zones did affect the formation of the fine wear debris, but the effect of coating discontinuities on the formation of the fine wear debris was dominant as a higher number density of localized pores was located within the scratch path. That is to say, it showed a size dependence. In the

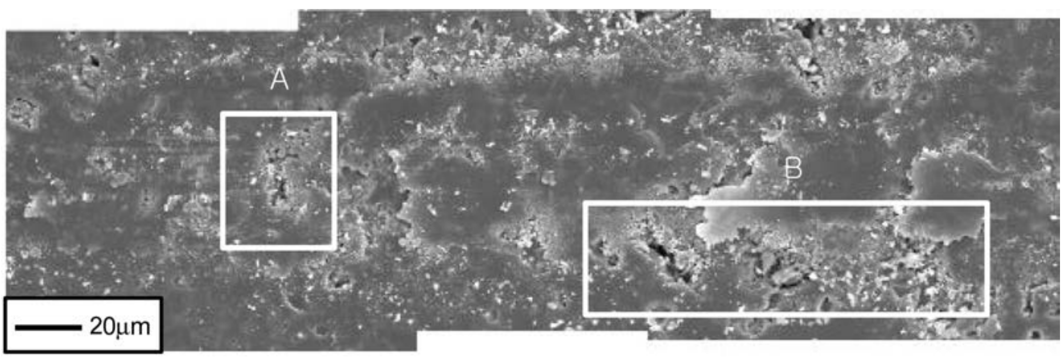

Fig. 8. Fine wear debris along a scratch.

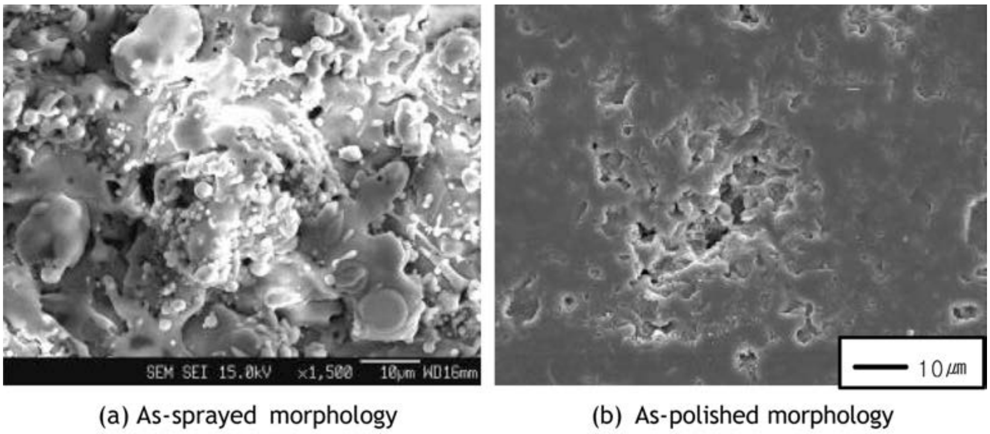

Fig. 9. Improperly flattened zone in the APS coating.

case of an isolated fine discontinuity, such as a pore, it seemed to be easily closed by the applied stress-induced inelastic mass flow during scratching. However, a discontinuity having a relatively higher localized pore population, as shown in Fig. 8 at B, enhanced the fine debris formation.

An improperly flattened zone, largely affecting the formation of the fine debris, is shown in Fig. 9. Where (a) is the morphology of the as-sprayed surface and (b) is the that of the as-polished surface. From the view-point of the morphology, this kind of coating discontinuity resulted from the splashing of the impacting molten particles. There were indeed a large number of satellite particles resulting from this splashing to form the local pile-ups. If subsequent impacting molten particles did not fill the interstices of these localized pile-ups, a resulting porous discontinuity was left in the coating as shown in (b).

When the coating was exposed to a low applied load with a larger number of scratch cycles as shown in Fig. 10(a), the weight loss of the coating was mainly due to the formation of fine wear debris arising from grain crushing. As this number was increased, the wear particle size also increased. On the other hand, the weight loss of the coating showed a somewhat different behavior during cyclic scratching under higher normal loads. In addition to the formation of fine wear debris, it required 10 repeated scratch cycles before severe microcracking occurred. This premature failure was also accompanied by the large fragmented flake-like

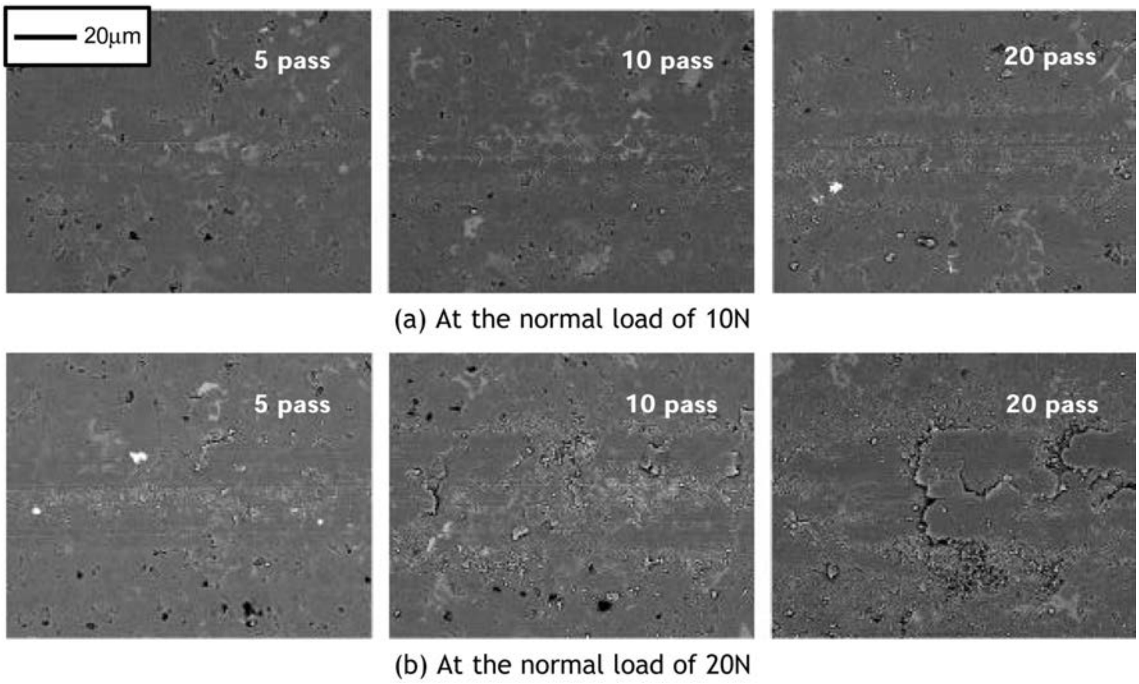

Fig. 10. BSE images of scratch according to the scratch condition.

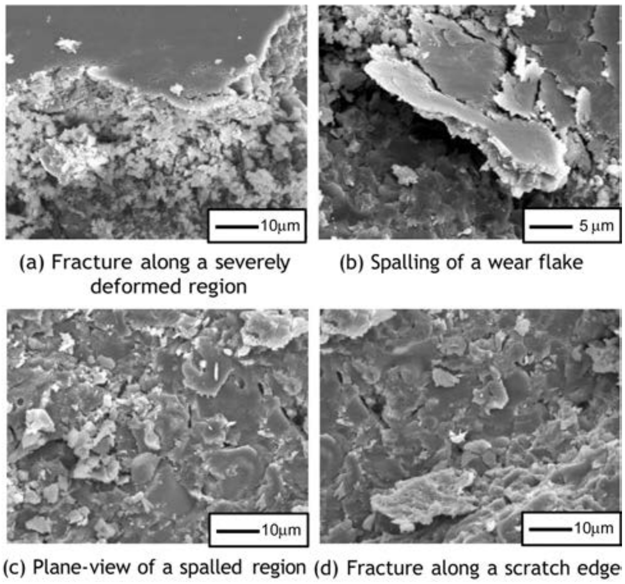

Fig. 11. Behavior of the flake-like spallation due to the repeated scratching.

wear debris due to partial spallation. For further scratch cycles, the spalled area radically increased to reach the whole span of the scratch width.

Under a high normal load after a critical number of scratch cycles, flake-like spallation was the dominant process for weight loss. Closer examination of the spalled areas was conducted as shown in Fig. 11. Through the presence of a higher density of fragmented fine particles near the severely deformed region, fracture was due to interlinking of a large number of microcracks during repeated scratch cycles (a). Image (b) shows the typical morphology of a spalled flake resulting from repeated scratch cycles. The morphology of the spalled flake seemed to be that of a highly deformed splat. The surface morphology at the spalled region, (c), implied that the flake spallation, as shown in (b), had been caused through the propagation of horizontal cracks along the splat boundaries: the smooth surface is the splat surface while the fine facet is a fractured splat where intimate contact was achieved. Dissimilar to the severely deformed region (a), sharp cracking could be observed around the scratch edge in (d).

While discontinuities, such as the improperly flattened zones, were the main defect in the formation of fine wear debris, intersplat pores and vertical cracks in the splat seemed to be critical defective structures for the formation of flake-like wear debris. Similar to a sintered alumina body [15-17], alumina-titania APS coatings show damage accumulation behavior. However, while the formation of the shear faults and microcracks were the major reason for the damage accumulation process in the sintered body, the intersplat pores due to the poor contact of the impacting particles were the main reason for damage accumulation in the APS coatings. That is to say, flake-like wear debris based on microcracking and fractures resulted from the propagation of the microcracks along the intersplat boundaries during repeated scratch cycles because of the lower cohesive strength due to poor contact between splats. In addition, stress could be concentrated at the intersplat pores and they also acted as pre-existing cracks for the fracture process.

Cross sections of the as-scratched specimens were prepared to investigate the damage accumulation process during repeated scratching.

Conclusion

Through this study, we could observe the effects of the scratching load and number of scratch cycles on the morphological changes in APS alumina-titania coatings. The following conclusions were obtained.

1) During scratching, the alumina-titania APS coatings showed fatigue behavior. That is to say, microcracking and fractures on the scratch path resulted from an accumulation due to the repeat number of scratch cycles.

2) A transition from plastic deformation to fracture was enhanced by an increase of the applied normal load.

3) The presence of coating discontinuities fostered formation of fine wear debris.

4) Spalled flake-like wear debris was due to subsurface damage accumulation during repeated scratch cycles and intersplat pores played a critical role in spalling.

Acknowledgement

This research was performed with the financial support of “The Ceramic Processing Research Center” under “Development of NT Ceramics technology Programs” of the Ministry of Science and Technology, Korea. We also thank Professor Lee, Jungjung at Seoul national university for the help in using the scratch tester.

References

1. B.S. Susan, H. Eschnauer, P. Huber, and A.R. Nicoll, Proc. 2nd plasma-technik-symposium, 1 (1991) 17, Lucerne, Switzerland.
2. M.I. Boulos, P. Fauchais, and E. Pfender, Thermal Plasmas, Plenum press, New York (1994).
3. P. Fauchais and A. Vardelle Heat, Interna. Jour. of Thermal Sci. 39 (2000) 852-870.
4. R. McPherson, Surf. and Coat. Tech. 39-40 (1989) 173-181.
5. L. Pawlowski, The Science and Engineering of thermal spray coatings, John Wiley & Sons, England (1995).
6. Y. Yang, Z. Liu, C. Luo, and Y. Chuang, Surf. and Coat. Tech. 89 (1997) 97-100.
7. L.C. Erickson, H.M. Hawthorne, and T. Troczynski, Wear

250 (2001) 569-575.
8. H.J. Kim, J. of the Korean Inst. of Met. and Mater. 27 (1989) 881.
9. K. Ramachandran, V. Selvarajan, P.V. Ananthapadmanabhan, and K.P. Sreekumar, Thin solid films 315 (1998) 144-152.
10. B. Normand, V. Fervel, C. Coddet, and V. Nikitine, Surf. and Coat. Tech. 123 (2000) 278-287.
11. L.C. Erickson, R. Westergard, U. Wiklund, H.M. Hawthorne, and S. Hogmark, Wear 214 (1998) 30-34.
12. Y. Xie and H.M. Hawthorne, Wear 225-229 (1999) 90-103.
13. Y. Xie and H.M. Hawthorne, Wear 240 (2000) 65-71.
14. H.S. Choi, H.J. Kim, B.H. Yoon, and C.H. Lee, Surf, and Coat. Tech. 150 (2002) 297-308.
15. B.R. Lawn, N.P. Pdture, F. Guiberteau, and H. Cai, Acta. Metal. Mater 42 (1994) 1683.
16. F. Guiberteau, N.P. Padture, and B.R. Law, J. Am. Ceram. Soc. 77 (1994) 1825.
17. B.A. Latella, B.H. O'Connor, N.P. Padture, and B.R. Law, J. Am. Ceram. Soc. 80[4] (1997) 1027.